BNL-76936-2006-JA

THE ATMOSPHERIC RADIATION MEASUREMENT (ARM) MOBILE FACILITY (AMF) AND ITS FIRST INTERNATIONAL DEPLOYMENT: MEASURING RADIATIVE FLUX DIVERGENCE IN WEST AFRICA

Mark A. Miller*
Brookhaven National Laboratory, Upton, NY USA

Anthony Slingo
Environmental Systems Science Centre
University of Reading, UK

Submitted to
Bulletin of the American Meteorological Society

July 2006

Environmental Sciences Department/Atmospheric Sciences Division

Brookhaven National Laboratory
P.O. Box 5000
Upton, NY 11973-5000
www.bnl.gov

*Corresponding author: Mark Miller, Brookhaven National Laboratory, ASD/ Bldg. 490D, Upton, NY, 11973 (miller@bnl.gov)

Abstract

The Atmospheric Radiation Measurement (ARM) Mobile Facility (AMF) was recently developed to enable collection of detailed climate data in locations not currently sampled by ARMs five fixed sites. The AMF includes a comprehensive suite of active and passive remote sensors, including cloud radar, that sample the atmosphere in a narrow column above its location. Surface radiation, aerosols, and fluxes are also measured and there is an ancillary measurement facility to help quantify local gradients. The AMF is deployed at no cost to the principal investigator or institution for periods of six months to one year on the basis of an international proposal competition judged by a nonpartisan board. The proposal to ARM that led to the initial international deployment of the AMF in Niamey, Niger, Africa was titled "Radiative Atmospheric Divergence using the AMF, GERB data, and AMMA Stations (RADAGAST)". This paper provides a description of the instruments that compose the AMF, its charter, a description of its deployment in support of RADAGAST, and examples of data that have been collected in Africa.

1. Introduction

A primary goal of the US Department of Energy's Atmospheric Radiation Measurement (ARM) Program (Stokes and Schwartz, 1994; Ackerman et al., 2003) is to collect and analyze data that can be used to improve the representation of clouds and radiation in Global Climate Models (GCMs). The ARM program currently operates five fixed sites: three sites in the Tropical Western Pacific, an Arctic site on the North Slope of Alaska, and a mid-continent site in Southern Great Plains of the United States (Oklahoma). To complement these fixed sites, the ARM Program has recently developed the ARM Mobile Facility (AMF) to enable data collection in additional regions of interest to the general atmospheric science community. The AMF is designed to operate continuously for periods of six to twelve months and includes a core suite of active remote sensors that are similar to those at the fixed sites. Deployments are determined through an international proposal competition and data are freely distributed through the ARM archive (www.arm.gov), typically in near real time.

The purpose of this paper is to describe the AMF instrumentation and its charter as a Department of Energy Facility, and to demonstrate the use of the AMF in its first international field deployment in Niamey, Niger, Africa. This deployment is associated with two large international campaigns: the African Monsoon Multi-Disciplinary Analysis (AMMA; Lebel et al., 2003) and the Geostationary Earth Radiation Budget (GERB; Harries et al., 2005; Allan et al., 2005) experiment. The proposal to ARM that led to this initial international deployment was titled "Radiative Atmospheric Divergence using the AMF, GERB data, and AMMA Stations (RADAGAST)". It represents an international effort to continuously measure the radiative fluxes at the surface and top-of-the-atmosphere through the seasonal progression of the West African Monsoon, which is strongly impacted by Saharan dust, biomass burning, and the development of deep convection in association with the intertropical convergence zone.

2. Instrumentation

The AMF is designed to continuously sample cloud, aerosol, thermodynamic, and wind conditions in a relatively narrow column above the deployment location, and to measure the fluxes of radiation, latent heat, sensible heat, and carbon dioxide at the surface. The centerpieces of the AMF are a collection of active and passive remote sensors (Table 1) including a vertically pointing 95-GHz Doppler radar (3.2 mm wavelength), which provides a profile of effective reflectivity factor and a full spectrum of the Doppler velocities at each range gate (Lhermitte, 1987; Clothiaux, 1995; Kollias et al., 2006; Figure 1; Box 1). The operating frequency of this radar was selected to minimize unwanted echoes from insects typically observed at longer wavelengths and to enable advanced signal processing techniques that rely on unique radar backscatter characteristics when hydrometeors reach the proportions of drizzle (100 μm). The AMF 95-GHz Doppler radar is capable of detecting small cloud droplets with diameters of 5-10 μm due to its 3.2-mm wavelength and is sensitive enough to detect most clouds in the column with the exception of extremely thin cloud layers, particularly in the upper troposphere. It has a relatively narrow beamwidth (<1˚), resulting in a small sampling volume, and deployments of similar cloud radars over the past decade have produced optimized sampling configurations (Kollias et al., 2004). It is feasible in most circumstances to retrieve a credible cloud droplet spectrum in liquid clouds with a vertical resolution on the order of 30-m and a temporal resolution on the order of 2-sec. When clouds contain a bi-modal droplet distribution advanced signal-processing techniques can be applied. Determination of cloud microphysical properties in mixed-phase and ice clouds is less certain, though a subject of considerable research.

The location of the cloud base is fundamental to radiation transfer and cloud formation in the atmosphere. Cloud base is defined as the lowest level in the atmosphere at which the air contains a perceptible quantity of cloud particles (Glossary of Meteorology, 1989). An observer

using only a visual inspection of an isolated thick cloud in a broken cloud field will identify the "optical" cloud base as the location where there is noticeable bluish tint and a reduction in intensity of scattered diffuse radiation. The observer may not visually detect a few scattered drizzle or raindrops below the perceptible optical cloud base because they do not scatter enough visible radiation compared to the smaller cloud droplets. These falling particles represent a double edged sword because they typically have minimal direct impact on the diffuse or direct radiation at that moment, but may have an important impact on the overall radiative budget of the cloud system through their ability to reduce cloud liquid water. Detection of the optical cloud base height is difficult using a 95-GHz radar because of extreme sensitivity to drizzle-size and larger droplets that are often found in the vicinity of the optical base. Therefore, lasers are used to identify the optical cloud base and the 95-GHz radar to quantify the cloud water flux above, through, and below the optical cloud base.

A Micropulse Lidar (MPL) that transmits at a wavelength of 523 nm with a vertical resolution of 30-m is the primary cloud base detector for the AMF (Spinhirne, 1993; Campbell et al., 2002). A laser ceilometer operating in the near infrared wavelength band (905-nm) with a vertical resolution of 15-m serves as a back up to increase overall system reliability. The MPL can measure lowest cloud base heights even when they are high in the troposphere (18-km), while the laser ceilometer measures cloud base to approximately five kilometers. Laser backscatter profiles are recorded for both lasers and the profile from the MPL can be used in clear skies to map vertical aerosol structure.

The column-integrated water vapor and liquid water are measured by recording passive emissions from the atmosphere in the microwave region using a Microwave Radiometer (MWR; Liljegren et al., 2001; Westwater et al., 2001). All of the water molecules in the column emit in the microwave region of the electromagnetic spectrum, although different phases of water have

emission peaks in slightly different regions of the spectrum[1]. Research suggests that this technique is accurate when the liquid water path exceeds 20-30 gm^{-2} (Turner et al., 2006), though new algorithms may reduce this uncertainty in coming years.

Extra microwave frequencies are added to sample the detailed structure of the water vapor and oxygen emission (absorption) peaks, which ultimately contains information about the thermodynamic profile (Gary, 1988; Güldner and Spanküch, 2001). At the center of an absorption line, the microwave emission is strongly weighted toward the lowest levels of the atmosphere, while incremental excursions on either side of the absorption line are weighted toward increasingly higher levels in the atmosphere. Adding four additional frequencies around 22-GHz enables low-resolution vertical profiles of the water vapor to be obtained through mathematical inversion of a set of equations and the use of a radiation transfer model. Sampling the structure of the oxygen absorption line with additional frequencies in the region between 50 and 60-GHz provides a low-resolution temperature profile because the temperature of the atmosphere determines the oxygen emission. The AMF has a twelve-channel MWR profiler (MWR-P) whose vertical resolution varies according to the atmospheric conditions.

An Atmospheric Emitted Radiance Interferometer (AERI) measures the infrared emission spectrum in great detail (Feltz et al., 1998). Applications of the AERI include derivation of thermodynamic profiles, cloud microphysical properties, and specific information about the composition of atmospheric constituents, such as dust (Smith et al., 1999; Collard et al., 1995; Turner et al., 2004). Thermodynamic profiling in clear skies is accomplished in a manner similar to the MWR, where the detailed shape of an emission line is used to provide information about the vertical structure of the atmosphere. In cloudy skies, the Atmospheric Emitted Radiance

[1] The emission spectra of water vapor and liquid water have considerable overlap, but water vapor is more dominant in the vicinity of 22-GHz (location of a water vapor absorption band) and liquid water in the vicinity of 31-GHz (location of a minimum in water vapor absorption). Simultaneous measurements of the emissions in these two channels produce two equations and two unknowns that can be solved to produce estimates of the column-integrated water vapor and liquid water.

Interferometer can be used to compute the liquid water path when clouds are too thin to overcome the noise level and uncertainty of microwave radiometer measurements. Specific regions within the infrared spectrum are also associated with characteristics of the cloud droplet spectrum (Turner et al., 2005; Lubin and Vogelmann, 2006).

A three-beam Doppler UHF profiler (915 or 1036 MHz frequency, depending on deployment location) is used to measure the wind structure to a range of five kilometers with 75-m vertical resolution (Ecklund et al., 1988). The scattering targets for this radar are mainly clusters of water molecules that are spaced geometrically in a manner that enables the microwave radiation transmitted from the radar to experience constructive interference when it is scattered (Bragg scatter), thereby boosting the received power level at the radar antenna. These clusters of water molecules are associated with turbulent eddies imbedded in the larger scale flow and are thus tracers of the wind. The Doppler velocity of these clusters is measured along three beams required to measure the horizontal and vertical wind flow: a zenith beam and two off-zenith beams (15˚) that are perpendicular to one another. This UHF radar can also measure the fall velocity of raindrops during precipitation (Gossard et al., 1982; Gossard et al., 1988).

Broadband downwelling irradiance is measured at the surface using standard pyranometers. A solar tracker is used to shade the solar disk on one pyranometer, thereby yielding the diffuse irradiance, and a Normal Incidence Pyroheliometer mounted on the tracker simultaneously measures the direct component of the irradiance. A complementary set of unshaded pygeometers measures the total broadband irradiance. Spectral components of the shortwave direct, diffuse, and total irradiances are measured using a Multiple-Frequency Shadowband Radiometer (MFRSR), which dissects the irradiance into seven narrow bands, each of 10-nm width (Harrison and Michalsky, 1994a,b). These bands can be used to retrieve information about aerosol particle size, ozone and water vapor absorption. Coincident broadband longwave measurements are

made by shaded and unshaded pyrgeometers (no measurement of the normal incidence is attempted).

Upwelling shortwave and longwave irradiances are measured using pyranometers and pyrgeometers that are identical to those used to make the downwelling measurements, although no shading is required (Table 2). The upwelling radiometers are mounted approximately 2-m above the surface and are particularly susceptible to local influences because surface conditions may vary widely over the region where the AMF is deployed. An ancillary surface radiation package described later is occasionally deployed to ameliorate this problem and to provide additional information that can be used to evaluate local influences that may be present in the AMF surface radiation data.

Two additional sensors provide information about the state of the sky and the infrared temperature of the atmospheric column above the AMF location. A Total Sky Imager (TSI) captures a digital image of the sky condition every 30-seconds during the daylight hours (Long and DeLuisi, 1998). This image is analyzed to determine the cloud coverage and to provide a qualitative description of the clouds that are present in the column (percent of opaque and thin clouds). A narrow-beam Infrared Thermometer (IRT) measures the temperature at cloud base when the clouds are thick enough to radiate as a blackbody.

Surface latent and sensible heat fluxes and the carbon flux are measured by an eddy correlation system (Webb et al., 1980; Moore, 1986). The area of the land surface represented by these flux measurements (footprint) is determined by the atmospheric state, surface conditions, and measurement height above the surface (Leclerc et al., 1997; Schuepp et al., 1992), so the eddy correlation system is mounted a height that is consistent with the scientific objectives of the deployment. Standard surface meteorological variables, including rainfall rate (liquid water flux) and surface visibility, are also measured at the surface.

The AMF has an Aerosol Observing System designed to measure the visible light aerosol scattering and absorption coefficients, as well as the cloud-nucleating characteristics of aerosols near the surface (Figure 2, Table 3). Aerosols and cloud droplets are collected from an inlet located 10-m above the surface and sorted into two size ranges: particles with a radius greater than 5 μm and particles less than 5 μm. This enables both cloud water (>5 μm radius) and interstitial (< 5 μm radius) aerosols to be sampled, regardless of the situation (i.e., presence or absence of fog or cloud).

Nephelometers measure, at more than one angle, the scattering properties of aerosol and cloud particles, while a Particle Soot Absorption Photometer measures the amount of visible radiation absorbed at set wavelengths. These instruments provide measurements of the aerosol single scattering albedo, asymmetry parameter, mass scattering efficiency, and hygroscopic particle growth that can be used in calculations of aerosol radiative forcing[2] (Anderson and Ogren, 1998; Anderson et al., 1999; Bond et al., 2001). The absorption, total scattering, and backscattering coefficients are measured coincidently at 450 nm ± 50 nm, 550 nm ±50 nm, and 700 nm, thereby providing an estimate of the extinction coefficient, which is the sum of the absorption and scattering coefficients. The aerosol measurements are also made through a range from 40-90% relative humidity to provide indication of the amount of water absorbed by the aerosol as a function of relative humidity (hygroscopic growth factor), which depends on the aerosol size and chemistry. This information is necessary to estimate the scattering coefficient at the ambient humidity.

The aerosol activation curve[3] is measured over a 30-minute period through an adjustable supersaturation range (0.018 to 1.37 are currently used) through which a total of seven supersaturation set points are sampled. The aerosol activity curve is related to the in-cloud

[2] Radiative forcing is defined as the radiative heating or cooling effect of aerosol on the atmosphere.
[3] the number of condensation nuclei that act as cloud condensation nuclei as a function of the supersaturation

updraft velocity because higher updraft velocities produce larger supersaturations, which in term activates progressively smaller aerosol particles.

All data collected using the AMF core instruments are made available to the public in near-real time. Data are transferred to a data management facility where instrument status is monitored and initial quality control is performed and files are converted to a standard format (NETCDF). Certain data streams are subjected to higher level processing to produce additional geophysical variables prior to release and efforts are made to release data for general use as soon as possible.

3. Site selection process

The AMF is deployed for periods ranging from six months to one year through an international proposal competition that is judged by the ARM Climate Research Facility Board. This board is comprised of four members from the ARM Science Team, excluding the AMF Site Scientist, and five members from other agencies, programs, and disciplines. This ensures that the AMF serves as a community facility and the deployment locations support a broad range of scientific objectives. Proposals are solicited once per year and ranked by potential scientific impact, cost, operational feasibility, and potential leverage in the form of contributions to the proposed project by other entities.

4. The RADAGAST Project: the first international deployment of the AMF

The AMF was initially deployed for six months at Pt. Reyes National Seashore, California in support of the Marine Stratus Radiation, Aerosol, and Drizzle Experiment (MASRAD; Miller et al., 2005). Subsequently, a proposal entitled RADAGAST (Radiative Atmospheric Divergence using Arm mobile facility, Gerb data and Amma STations) was submitted to ARM by the second author and was selected for implementation. Under this project, the AMF is

deployed at Niamey, Niger, for the whole of 2006. The observations that contribute to this project are described below, but first we provide some background on the scientific motivation.

a. Scientific background to the RADAGAST experiment

Despite good progress over the last few decades in quantifying the physical processes that control the interaction of solar and thermal radiation with the atmosphere and surface, a number of important gaps in our understanding remain. These gaps are highlighted by disagreements between observations and numerical radiative transfer schemes. Clouds present some of the most difficult problems, which include the radiative properties of ice and mixed-phase clouds, as well as the quantification of 3-D effects (Cahalan et al., 2005). It is also recognized that aerosols make a substantial contribution to current uncertainties, not only through their direct effects on the radiation fields but also through their indirect effects on cloud microphysics and radiative properties. Both effects are extremely uncertain, because of the wide range of aerosol types and properties and the complexity of the interactions between aerosols, water drops and ice crystals (Haywood and Boucher, 2000). Even in clear skies, where progress has been particularly impressive for thermal radiation (Turner et al., 2004), there are discrepancies which are compounded by the complex spectrum of water vapor absorption, which includes thousands of weak spectral lines and a strong underlying continuum, neither of which have yet been fully quantified (Pilewskie et al., 2000; Ptashnik et al., 2004).

In addition to the specific process problems mentioned above, there are more general difficulties in reconciling long-term satellite measurements of the radiation budget at the top of the atmosphere with direct measurements of radiative fluxes at the surface and with models. Radiative fluxes at the top of the atmosphere are now well observed from satellites. In contrast, fluxes at the surface are less well observed, due to the variable quality and sparse distribution of measurements. As a result, estimates of the radiation balance of the atmosphere are not well

constrained. For example, estimates of the global absorption of solar radiation vary from 67 to 98 Wm^{-2} (Kiehl and Trenberth, 1997; Wild, 2005). The more recent estimates suggest that the atmosphere is more absorbing and this leads to major problems when comparisons are made with models. It is relatively straightforward to tune a climate model to produce agreement with the observed globally averaged radiative fluxes at the top of the atmosphere, to within the errors in the satellite data. However, for most climate models there are substantial disagreements when the comparison is then made at the surface. Models typically produce too much downward solar radiation and too little downward thermal radiation at the surface, compared with the measurements (Wild et al., 2006; Wild et al., 2001). This implies that the modeled atmosphere is too transparent and in particular that the atmosphere absorbs significantly more solar radiation than can be accounted for in most current models.

Several independent studies have arrived at this conclusion, which appears to be robust, despite the uneven distribution of surface observations including a complete lack of data over much of the oceans (Gilgen and Ohmura, 1999). Explanations of these results in terms of additional or excess solar absorption by clouds have been extremely contentious (Valero et al., 2004; Li et al., 2004) and no consensus has yet been reached on this problem. It is possible that absorbing aerosols may be making a contribution (Wild, 2005), which emphasizes again the value of the measurements being made in Niamey.

Attempts to resolve the problems outlined above through field experiments have been beset by sampling problems. These problems include the limited global distribution of surface sites and limited instrumentation, the limited spatial and temporal sampling by in situ experiments using aircraft, and the limited spatial, temporal and/or spectral sampling by satellites above the few well-instrumented surface sites. In order to minimize the sampling problems, an extended series of broadband observations from both space and the surface are required, with high

temporal resolution. This in effect means a combination of a geostationary satellite and a well-instrumented surface site, which are the essential components of RADAGAST.

b. Components of RADAGAST

The choice of site for the AMF deployment was determined partly by the fact that Niamey is the center of operations for the Special Observing Periods of the AMMA project in 2006. AMMA seeks to improve understanding of the West African monsoon and its impact on both the local and global climate (Lebel et al., 2003). Niamey is an excellent site for the deployment given the opportunities provided by the seasonal changes in meteorological conditions, the wide experience in working in this region and the detailed logistical planning taking place for AMMA. The meteorological conditions experienced at Niamey include deep tropical convection in the wet season and episodes of mineral dust (from the Sahara) and biomass burning aerosols in the dry season. The Sahara is the most important source of desert dust aerosols on Earth (Prospero and Lamb, 2003) and the water vapor loading changes dramatically between the wet and dry seasons (Figure 3). The divergence of atmospheric radiation through deep convection and aerosol are still poorly understood and this deployment will enable a concerted attack on these problems. The AMMA field phases extend over 2005-07 (including networks of surface flux measurements and some surface aerosol observations), with the main intensive observations in 2006 (January 2006 to September 2006). In particular, the DABEX (Dust and Biomass Experiment) employed both aircraft and surface sites in a very successful study of dust and biomass aerosol in the region during January 2006.

The Niamey site is also in a favorable position for coordinated observations with the Meteosat series of operational geostationary satellites. The current satellite, known as Meteosat-8, carries the Geostationary Earth Radiation Budget (GERB) instrument, which is the first broadband radiometer to fly on a geostationary satellite (Harries et al., 2005; Allan et al., 2005).

GERB observes the radiation budget with the unprecedented temporal resolution of 15 minutes: the same as the high resolution Spinning Enhanced Visible and Infra-Red Imager (SEVIRI) on the same satellite (Schmetz et al., 2002). Further GERB and SEVIRI instruments will fly on the following three satellites in this series. The first of these, Meteosat-9, was launched in December 2005 and is expected to become the operational satellite in August 2006. For the RADAGAST project, data from the AMF will be merged with those from AMMA, GERB and SEVIRI to provide a dataset that describes the surface and top-of-atmosphere radiative fluxes and the structure of the atmosphere between.

The data collected during RADAGAST will be especially valuable for evaluating climate and NWP models. In addition, there are many other projects that could benefit from the new data. These include the evaluation of surface fluxes derived from satellite data, studies of the radiative properties of water vapor, aerosols and clouds, the diurnal cycle, and the structure of cloud and aerosol layers. The AMF became operational at the beginning of 2006 and is planned to operate continually throughout the year.

c. Details of the deployment in Africa

The Niamey Airport was chosen as the most appropriate location for the AMF to meet RADAGAST science objectives and for various logistical reasons (Figure 4a). The photographs show the location of the main AMF equipment vans and the instrument stands. No structural modifications were made to the existing buildings. The AMF deployment, although primarily self sufficient, is reliant on grid power (backed up by a standby generator). Data are transmitted to Niamey by a wireless link and subsequently to the main ARM archives. Data from the second site (see below) are logged locally and collected every week.

The instrument vans in the main site are individually air conditioned and connected together by a tent that provides protection from blowing dirt, minimizes the loss of air

conditioning when the van doors are opened, and provides additional security. Various instruments mounted on stands are located a hundred meters or so from the vans (Figure 4b). While logistically convenient, the location of the site is quite close to the airport buildings and aircraft taxiways. This location may affect some of the measurements at certain times although no major problems have been encountered to date. A second, remote site was therefore established near Banizoumbou (Figure 5), using solar power. This includes a more limited range of instrumentation to measure basic meteorological fields and broadband fluxes. This site is representative of a large area of this part of the Sahel and so the observations will be of particular importance, as well as providing a comparison with the measurements from the airport site.

d. Selected Results

The goal of RADAGAST is to measure the fluxes at the surface using the AMF and at the top-of-the-atmosphere using GERB and SEVIRI. These boundary conditions enable, in principle, a direct measurement of the radiation absorption properties of the atmosphere, although the difference in scale between the satellite pixels and the essentially point measurements at the surface needs to be addressed. The radiative absorption characteristics of dust and biomass burning aerosol in the region are of particular interest. Data collected on 23 January 2006 are rather typical of the boundary layer aerosol in the vicinity of Niamey. Cross-sections from the AMF Micropulse lidar show a stratified layer of aerosol from the surface to nearly 5-km (Figure 6). Aircraft penetrations of similar aerosol layers during DABEX show that the lowest 2-km usually contains a mixture of dust and biomass burning aerosol, while the layer from 2-5-km is predominantly comprised of biomass burning aerosol (Haywood, personal communication).

Cirrus and mid-level clouds are often observed in the vicinity of Niamey as the monsoon develops, as indicated by time-height cross-sections from cloud radar collected on 26 April 2006

(Figure 7). Data from the cross-polarization channel of this radar suggest that the cirrus clouds (8-14 km) are composed of irregularly shaped ice crystals, while the mid-level clouds (2-6 km) and their precipitation shafts are likely to be mixed phase. Soundings taken during the day reveal complex vertical structure with a well-mixed boundary layer with little wind to approximately 3-km. The layer from the top of the boundary layer to the tropopause has winds with south or southwest component and is relatively moist. It is periodically saturated in thin layers, especially from 3-5 km and from 8-14 km.

Data collection in Niamey will continue through the end of 2006. Calculations of the profile of atmospheric heating profile for RADAGAST require specification of the profiles of clouds and aerosols, along with standard thermodynamic data, so the AMF data presented above represent the path forward toward the longer-term goal of better understanding of the profile of atmospheric heating in West Africa.

5. **Summary**

The AMF is a powerful new resource for use by the international climate and atmospheric science community. Its design echoes that of the fixed ARM sites and benefits from over a decade of experience in collecting data sets that can be used to improve GCMs. It is deployed for periods of six to twelve months on the basis of a competitive proposal process and its initial deployments have drawn considerable interest in the international atmospheric science community. It is expected that the AMF will provide seminal data that can be used to improve the accuracy of GCMs in regions that are currently under sampled.

The combination of continuous, detailed information about the state of the atmospheric column from the AMF and continuous broadband radiation measurements from satellite in the vicinity of Niamey, Niger, Africa presented above represent a new paradigm for atmospheric science in that the surface and top-of-the-atmosphere broadband radiative fluxes and computed

heating rate profiles are available continuously over a diurnal cycle. Such observations have not been possible up to now, because all of the other satellites with broadband radiation sensors are in polar orbits, rather than geostationary.

The success of the first AMF has inspired planning for a second facility, to be built and deployed within the next 3-4 years. This new facility will have capabilities that complement the current facility and may include scanning sensors.

6. Acknowledgements

Many dedicated professionals have contributed to the design, construction, and deployment of the ARM Mobile Facility. Mike Alsop , Betsy Andrews, Mary Jane Bartholomew, Dick Egan, Larry Jones, Pavlos Kollias, Kim Nitschke, John Ogren, Rex Peterson, Doug Sisterson, Jimmy Voyles, and Kevin Widener have made notable contributions. We are also deeply indebted to our program manager at the Department of Energy, Dr. Wanda Ferrell and to Dr. Tom Ackerman, past ARM Chief Scientist, for their efforts to develop the AMF. We are grateful to Richard Allan for providing Figure 3. This manuscript has been authored by Brookhaven Science Associates, LLC under Contract No. DE-AC02-98CH10886 with the U.S. Department of Energy. The United States Government retains, and the publisher, by accepting the article for publication, acknowledges, a worldwide license to publish or reproduce the published form of this manuscript, or allow others to do so, for the United States Government purposes.

7. References

Ackerman, T.A. and G.M. Stokes, 2003: The Atmospheric Radiation Measurement Program, *Physics Today*, **56**, 38-45.

Allan, R. P., A. Slingo, S.F. Milton, and I. Culverwell, 2005: Exploitation of Geostationary Earth Radiation Budget data using simulations from a numerical weather prediction model: Methodology and data validation. *J. Geophys. Res.,* **110,** D14111, doi:10.1029/2004JD005698.

Anderson, T.L., D.S. Covert, J.D. Wheeler, J.M. Harris, K.D. Perry, B.E. Trost, D.J. Jaffe, and J.A. Ogren, 1999: Aerosol backscatter fraction and single scattering albedo: measured values and uncertainties at a coastal location in the Pacific Northwest, *J. Geophys. Res.,* **104,** 26793-26807.

Anderson, T.L. and J.A. Ogren, 1998: Determining aerosol radiative properties using the TSI 3563 integrating nephalometer, *Aerosol Sci. and Tech*., **29**, 57-69.

Bond, T.C., T.L. Anderson, and D. Campbell, 2001: Calibration and intercomparison of filter-based measurements of visible light absorption by aerosols, *Aerosol Sci. and Tech.*, **30**, 582-600.

Cahalan, R.F. and co-authors, 2005. The I3RC. Bringing together the most advanced radiative transfer tools for cloudy atmospheres. *Bull. Amer. Meteorol. Soc.*, **86**, 1275-1293.

Campbell, J.R., D.L. Hlavka, E.J. Welton, C.J. Flynn, D.D. Turner, J.D. Spinhirne, and V.S. Scott, 2002: Full-time eye safe cloud and aerosol lidar observation at the atmospheric radiation measurement program sites: instruments and data processing. *J. Atmos. Ocean. Tech*, **19**, 431-442.

Clothiaux, E.E., M.A. Miller, B.A. Albrecht, T.A. Ackerman, J. Verlinde, D.M. Babb, R.M.Peters, and W.J. Syrett, 1995: An evaluation of a 94-GHz radar for remote sensing of cloud properties. *J. Atmos.Ocean.Tech*., **12**, 201-229.

Collard, A.D., S.A. Ackerman, W.L. Smith, X. Ma, H.E. Revercomb, R.O. Knuteson, and S.C. Lee, 1995: Cirrus cloud properties derived from high spectral resolution infrared spectrometry during FIRE II. Part III: ground-based HIS results. *J. Atmos. Sci.*, 52, 4264-4275.

Ecklund, W. L., D. A. Carter, and B. B. Balsley, 1988: A UHF wind profiler for the boundary layer: Brief description and initial results. *J. Atmos. Oceanic Technol.,* **5,** 432–441.

Feltz, W.F., W.L. Smith, R.O. Knuteson, H.E. Revercomb, H.M. Woolf, and H.B. Howell, 1998: Meteorological applications of temperature and water vapor retrievals form ground-based Atmospheric Emitted Radiance Interferometer (AERI), *J. Atmos. Ocean. Tech*, **37**, 857-875.

Gary, B.L., 1988: Passive microwave temperature profiler, report JPL-D-5484, Jet Propulsion Laboratory, California Institute of Technology, 25 pp.

Gilgen, H. and Ohmura, A., 1999. The Global Energy Balance Archive. *Bull. Amer. Meteorol. Soc.*, **80**, 831-850.

Glossary of Meteorology, 1989: The American Meteorological Society, edited by R. E. Huschke, 638 pp.

Gossard, E. E., Chadwick, R. B., Neff, W. D., and Moran, K. P., 1982: The Use of Ground-Based Doppler Radars to Measure Gradients, Fluxes and Structure Parameters in Elevated Layers. *J. Applied Meteor.*, **21**: 211-226.

Gossard, E. E., 1988: Measuring drop-size distributions in clouds with a clear-air-sensing Doppler radar. *J. Atmos. Oceanic Technol.,* **5,** 640–649.

Güldner, J. and D. Spanküch, 2001: Remote sensing of the thermodynamic state of the atmospheric boundary layer by ground-based microwave radiometry, *J. Atmos. Ocean. Tech*, **18**, 925-933.

Harries, J. E. and coauthors, 2005: The Geostationary Earth Radiation Budget (GERB) Experiment. *Bull. Amer. Meteorol. Soc.*, **86**, 945-960.

Harrison, L., and J. Michalsky, 1994a: Automated multi-filter rotating shadow-band radiometer: an instrument for optical depth and radiation measurements. *Applied Optics*, **33**, 5118-5125.

Harrison, L., and J. Michalsky, 1994b: Objective algorithm for the retrieval of optical depths from ground-based measurements. *Applied Optics*, **33**, 5126-5132.

Haywood, J. and Boucher, O., 2000. Estimates of the direct and indirect radiative forcing due to tropospheric aerosols: a review. *Rev. Geophys.*, **38,** 513-543.

Kiehl, J.T. and Trenberth, K.E., 1997. Earth's annual global mean energy budget. *Bull. Amer. Meteorol. Soc.*, **78**, 197-208

Kollias, P., E.E. Clothiaux, B.A. Albrecht, M.A. Miller, K.P. Moran, and K.L. Johnson, 2004: The atmospheric radiation measurement program cloud profiling radars: an evaluation of signal processing and sampling strategies, *J. Atmos. Ocean. Tech*, **22**, 930-947.

Kollias, P., E.E. Clothiaux, M.A. Miller, B.A. Albrecht, G.L. Stephens, and T.P. Ackerman, 2006: Millimeter-Wavelength Radars-New Frontier in Atmospheric Cloud Research, *Bull. Amer. Met Soc*. (submitted)

Lebel, T., Redelsperger, J.-L., and Thorncroft, C., 2003: African Monsoon Multidisciplinary Analysis (AMMA) Project. *GEWEX News*, **13,** No. 4, 8-9, November 2003.

Leclerc, M.Y., S. Chen, and B. Lamb, 1997: Observations of large eddy simulation modeling of footprints in the lower convective boundary layer. *J. Geophys. Res.*, **102**(D8), 9323-9334.

Li, Z., Wiscombe, W., Stephens, G.L., and Ackerman, T.P., 2004. Response. *Science*, **305,** 1240

Long, C.N. and J.J. DeLuisi, 1998: Development of an automated hemispheric sky imager for cloud fraction retrievals. *Proceedings 10th Symposium on Meteorological Observations and Instrumentation*, Phoenix, AZ.

Liljegren, J.C., E.E. Clothiaux, G. Mace, S. Kato, and X. Dong, 2001: A new retrieval for cloud liquid water path using a ground-based microwave radiometer and measurements of cloud temperature. *J. Geophys. Res*., **106**, 14,485-14,500.

Lubin, D. and Vogelmann, A. M., 2006: A climatologically significant aerosol longwave indirect effect in the arctic. *Nature*, **439**, 453-456.

Lhermitte, R.M., 1987: A 94_GHz Doppler radar for cloud observations. *J. Atmos. Oceanic Tech.*, 4, 36-48.

Li, Z., Wiscombe, W., Stephens, G.L. and Ackerman, T.P., 2004: Response. *Science*, **305,** 1240.

Moore, C.J., 1986: Frequency response corrections for eddy correlation systems, Boundary Layer Met., **37**, 17-35.

Pilewskie, P., and co-authors, 2000: The discrepancy between measured and modeled downwelling solar irradiance at the ground: dependence on water vapor. *Geophys. Res. Lett.*, **27,** 137-140

Prospero, J.M. and Lamb, P.J., 2003: African droughts and dust transport to the Caribbean: Climate change implications. *Science*, **302,** 1024-1027

Ptashnik, I.V., Smith, K.M., Shine, K.P. and Newnham, D.A., 2004: Laboratory measurements of water vapour continuum absorption in spectral region 5000-5600 cm^{-1}: evidence for water dimers. *Q. J. R. Meteorol. Soc*., **130,** 2391-2408.

Schmetz, J., P. Pili, S. Tjemkes, D. Just, J. Kerkman, S. Rota, and A. Ratier, 2002: An introduction to Meteosat Second Generation (MSG). *Bull. Amer. Meteorol. Soc.*, **83**, 977-992.

Schuepp, P.H., J.I. MacPherson, and R.L. Desjardins, 1992: Adjustment of footprint correction for airborne flux mapping over the FIFE site, *J. Geophys. Res*., **97**(D17), 18455-18466.

Smith, W.L., W.F. Feltz, R.O. Knuteson, H.E. Revercomb, H.B. Howell, and H.M. Woolf, 1999: The reteival of planetary boundary structure using ground-based infrared spectral radiance measurements, *J. Atmos. Ocean. Tech*, **16**, 323-333.

Spinhirne, J.D., 1993: Micro pulse lidar. *IEEE Trans. Geoscience Remote Sensing*, **31**, 48-55.

Stokes, G.M. and S.E. Schwartz, 1994: The Atmospheric Radiation Measurement (ARM) Program: programmatic background and design of the cloud and radiation testbed. *Bull. Amer. Meteorol. Soc.*, **75**, 1201-1221.

Turner, D.D. and co-authors, 2004: The QME AERI LBLRTM: A closure experiment for downwelling high spectral resolution infrared radiance. *J. Atmos. Sci*., **61,** 2657-2675.

Turner, DD., 2005: Arctic mixed-phase cloud properties from AERI-lidar observations: Algorithm and results from SHEBA. *Journal of Applied Meteorology*, **44**: 427-444.

Turner, D.D. and co-authors, 2006: Optically thin liquid water clouds: their importance and our challenge, *Bull. Amer. Meteorol. Soc.*, (submitted)

Uppala, S.M. and co-authors, 2005: The ERA-40 re-analysis. *Q. J. R. Meteorol. Soc.*, **131**, 2961-3012.

Valero, F.P.J., Cess, R.D., and Pope, S.K., 2004: Disagreements over cloud absorption. *Science*, **305,** 1239.

Webb, E.K., G.I. Pearman, and R. Leuning, 1980: Correction of flux measurements for density effects due to heat and water vapour transfer. Quart. J. Royal Met. Soc., **106**, 85-100.

Westwater, E., Y. Han, M. Shupe, and S. Matrosov, 2001: Analysis of integrated cloud liquid and precipitable water vapor retrievals from microwave radiometers during the Surface Heat Budget of the Arctic Ocean project. *J. Geophys. Res.*, **106**, 32,019-32,030.

Wild, M., Ohmura, A., Gilgen, H., Morcrette, J.-J., and Slingo, A., 2001: Evaluation of downward longwave radiation in general circulation models. *J. Clim*., **14,** 3227-3239

Wild, M., 2005: Solar radiation budgets in atmospheric model intercomparisons from a surface perspective. *Geophys. Res. Lett.*, **32,** L07704, doi:10.1029/2005GL022421

Wild, M., Long, C.N., and Ohmura, A., 2006: Evaluation of clear-sky solar fluxes in GCMs participating in AMIP and IPCC-AR4 from a surface perspective. *J. Geophys. Res.*, **111**, D01104, doi:10.1029/2005JD006118.

Table 1. Profiling and narrow beam column-integrating instruments that comprise the AMF

Instrument	Measurement	Resolution	Comments
95-GHz Cloud Radar (WACR)	effective reflectivity Doppler spectrum	range: 30m temporal: 2s	minimum detectable signal: -50 dBz at 2 km
Micropulse Lidar (MPL)	backscatter intensity: 523.5 nm	range: 30 m time: 30-60 s	maximum height: 18 km
Microwave Radiometer (MWR)	brightness temperature (5 channels), cloud liquid water path, precipitable water vapor	time: 20 s	minimum detectable cloud liquid water path: 20-30 gm^{-2}
Profiling Microwave Radiometer (MWR-P)	brightness temperature (12 channels), cloud liquid water path, temperature and water vapor profiles	time: 5 min range: variable	Range resolution dependent on atmospheric conditions
Atmospheric Emitted Radiance Interferometer (AERI)	absolute infrared spectral radiance in 1.3 degree field-of-view; temperature and vapor profiles	spectral: 3-19.2 microns with 3.3-36 nm resolution time: 6 min	temporal resolution will be improved to 20 s in near future
Laser Ceilometer	cloud base height, backscatter intensity	range: 15 m time: 30 s	maximum height is ~5.5 km
1040 MHz Wind Profiler	wind profile, precipitation Doppler velocity spectrum	time: 6 min resolution: 75 m	3 beams
Rawindsondes	pressure, temperature, relative humidity, winds	time: minimum of every 4 hours	moisture profile humidity profile scaled by MWR

Table 2. Surface flux, sky condition, and surface meteorological instruments used in the AMF

Instrument	Measurement	Resolution	Comments
Downwelling Radiation (SKYRAD)	Direct, diffuse, and global broadband shortwave (solar), longwave (infrared), irradiances for downwelling components.	Time: 1 min	included in ancillary facility
Upwelling Radiation (GNDRAD)	Broadband shortwave (solar) and longwave (infrared) irradiances	Time: 1 min	deployment height typically 2-m
Multi-filter Rotating Shadowband Radiometer	Aerosol optical thickness, aerosol Angstrom Exponent, cloud optical thickness	Time: 20 s	Channels: 415, 500, 615, 673, 870, 940 nm with 10 nm width, and a broadband channel
Infrared Thermometer (IRT)	Cloud base temperature	Time: <1 min	Cloud must be a blackbody (emissivity = 1)
Total Sky Imager	hemispheric sky images for daylight hours	Time: ~30 s	solar elevation > 5 to 10 degrees
Eddy Correlation	surface turbulent fluxes of momentum, sensible heat, latent heat	Time: one-half hour	Mounted at height determined by surface characteristics
Surface Meteorology	surface wind speed and direction, temperature, relative humidity, barometric pressure, rain-rate, and visibility	Time: 1 min	Mounted on 10-m tower in 2007

Table 3. The AMF Aerosol Observing System

Instrument	Description of Measurement	Comments
Integrating Nephelometer (operated at low RH):	Total scattering between 7˚ and 170˚ and backscattering between 90˚ and 170˚ at a relative humidity of 50%	Three measurement wavelengths: blue (450 nm), green (550 nm) and red (700 nm)
Integrating Nephelometer (operated at high RH scanned from ~40-90%)	Total scattering between 7˚ and 170˚ and backscattering between 90˚ and 170˚ at relative humidities scanned from ~40-90%)	Three measurement wavelengths: blue (450 nm), green (550 nm) and red (700 nm)
Particle/Soot Absorption Photometer	Filter-based method that measures light absorption by particles	Three measurement wavelengths: blue, green (565 nm), and red
Condensation Nuclei Counter	Total number concentration of condensation particles	Size range of 10 nm to 3 μm
Multiple-Supersaturation Cloud Condensation Nuclei Counter	Total number of cloud condensation nuclei as a function of supersaturation	six different adjustable supersaturations (currently 1.018 to 1.37)

Box #1:

Use of the full spectrum of Doppler velocities for cloud microphysics research

The AMF cloud radar continuously points toward zenith such that it measures the fall velocity of hydrometeors, which can be directly related to droplet size if the droplets are liquid or ice spheres. Cloud microphysical variations and turbulent motions within the cloud require detailed information about the distribution of the fall velocities in the cloud. To satisfy this requirement, the entire spectrum of fall velocities (or the Doppler velocity spectrum) in a given sample volume within the cloud is recorded continuously. This velocity spectrum may be used to separate the echoes from cloud droplets, which may have an upward velocity, from precipitation, which always has a downward velocity. The recording of this information enables data from the cloud radar to be analyzed in the context of the detailed microphysical process that are occurring within the cloud.

Figure 1. The AMF 95-GHz Doppler Radar

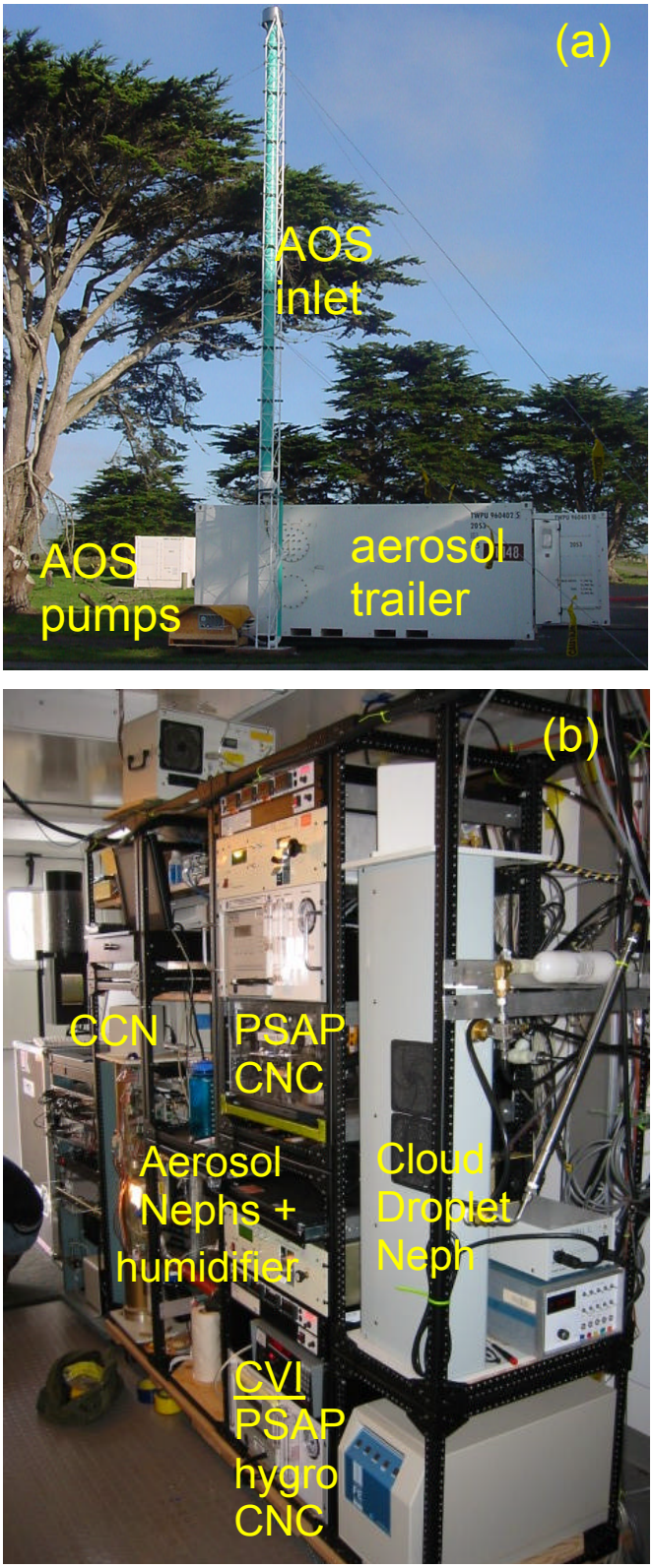

Figure 2. (a.) An external view of the AMF Aerosol Observing System showing the van housing the system, the 10-m inlet stack, and the pumps that are used to draw aerosol samples. (b) Inside the van showing the controls for the Counterflow Virtual Impactor (CVI) used to sort incoming aerosol particles by size, nephalometers (denoted Neph) for aerosol and cloud droplets, the Particle Soot Absorption Photometers (PSAP) for dry (40% relative humidity) and moist (40-90% relative humidity, the hygroscopic Condensation Nuclei Counters (CNC) for each PSAP, and the humidifier.

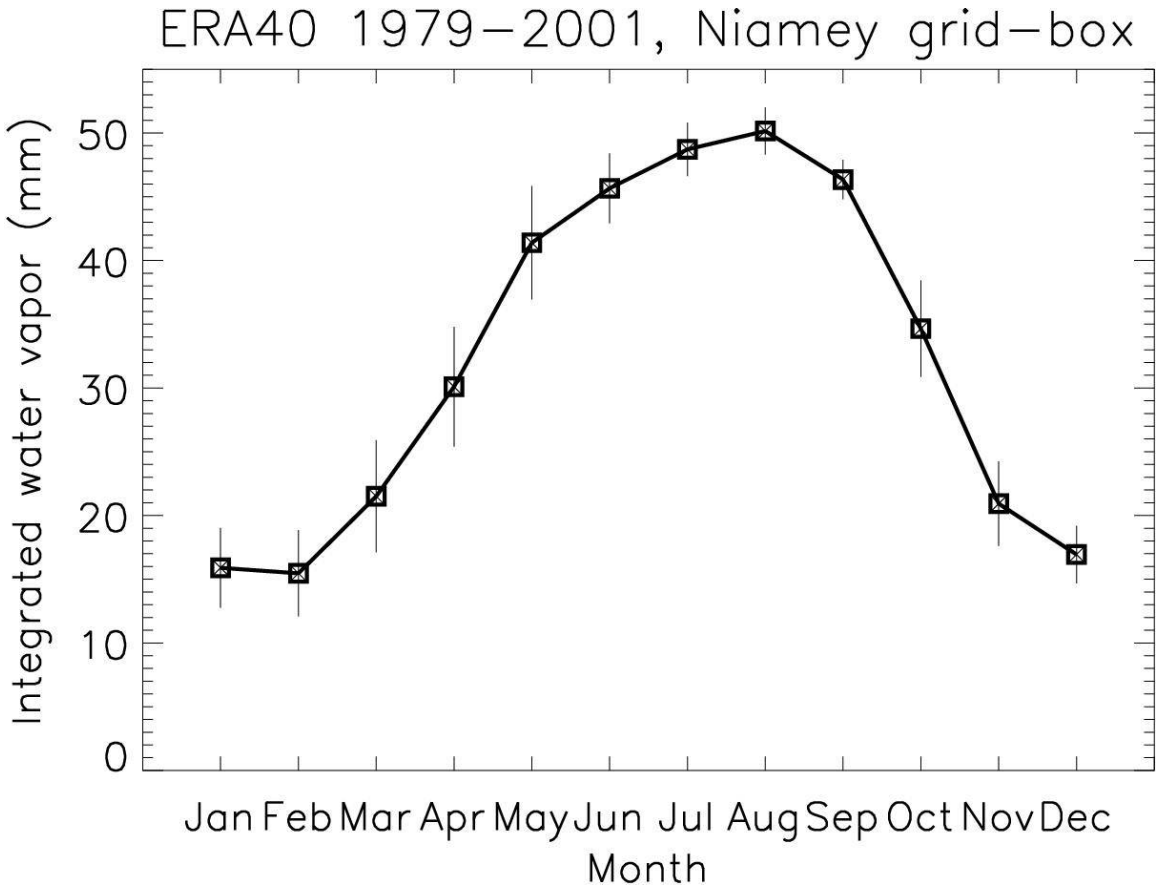

Figure 3. Monthly mean integrated water vapor in the atmospheric column over Niamey, averaged from 1979 to 2001, from the ECMWF 40-year re-analysis (Uppala et al., 2005). The maximum value during this period was 54.9 mm (July 1979) and the minimum value was 9.7 mm (January 2001). Daily variations extend over an even larger range.

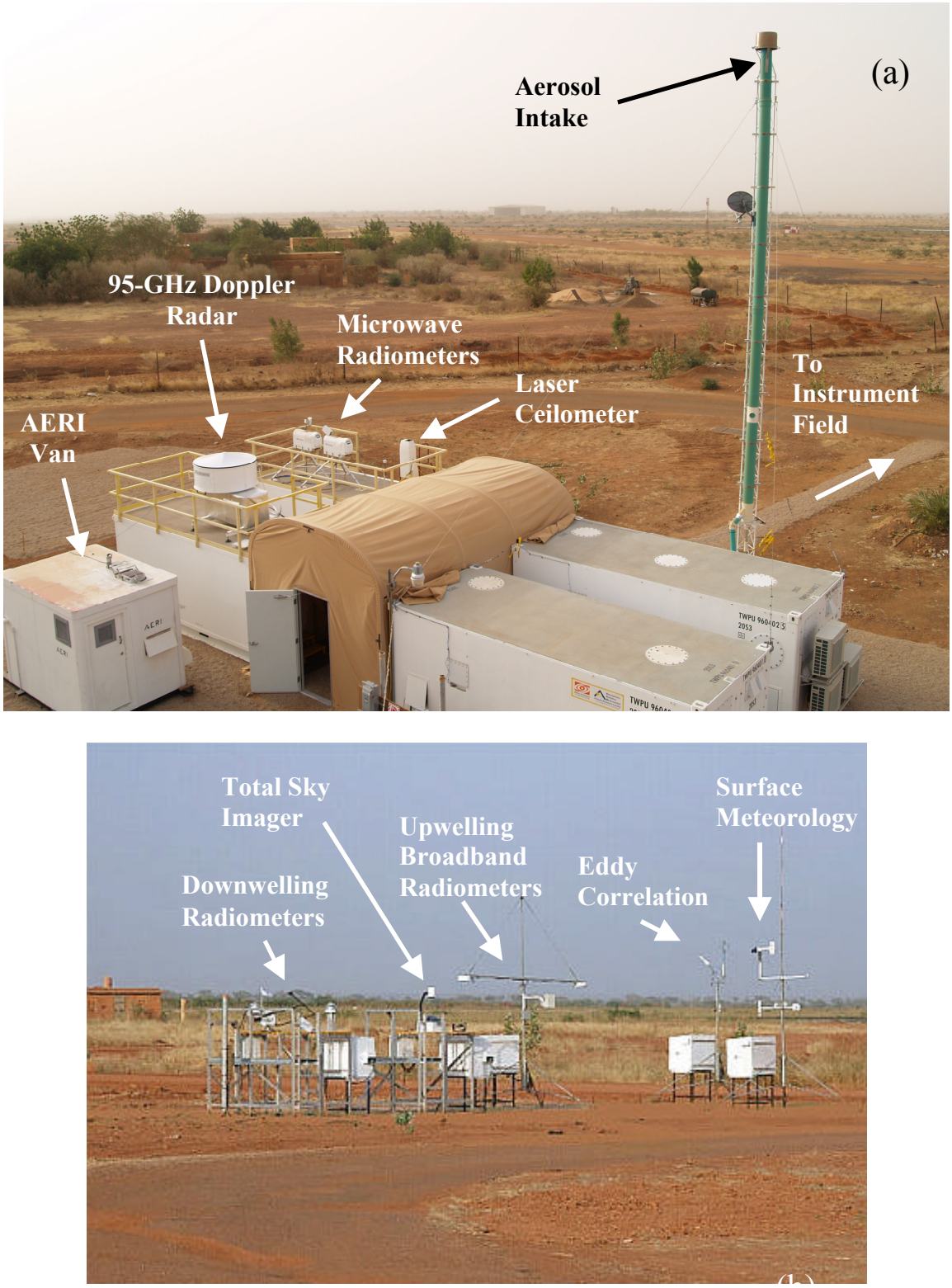

Figure 4. (a) Overview of the AMF site in Niamey, Niger Africa, and (b) the associated instrument field located approximately 100 m from the main facility

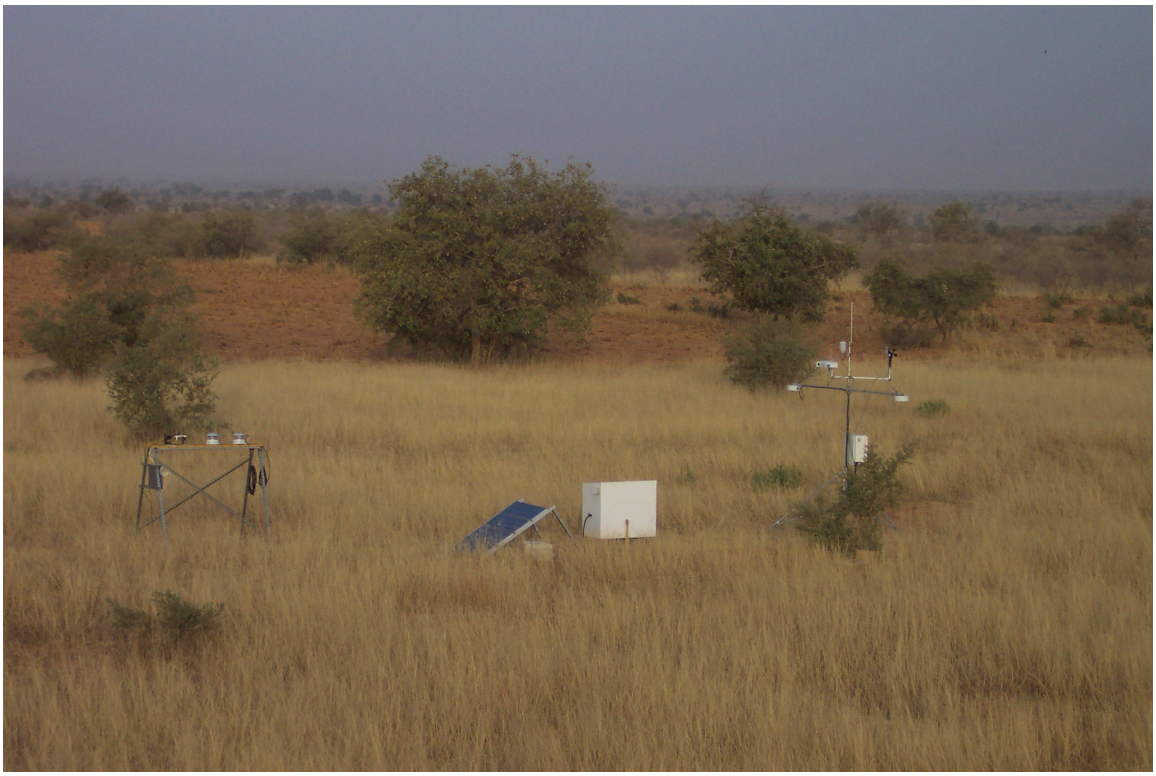

Figure 5. The AMF ancillary site at Banazambou, Niger, Africa. Broadband downwelling radiation is measured on the platform on the left-hand side of the picture and broadband downwelling on the lateral beam attached to the pole on the right-hand side of the picture. Standard meteorological variables are measured atop the pole on the right-hand side of the picture and the solar panel that provides power is the tilted silver plate in the center.

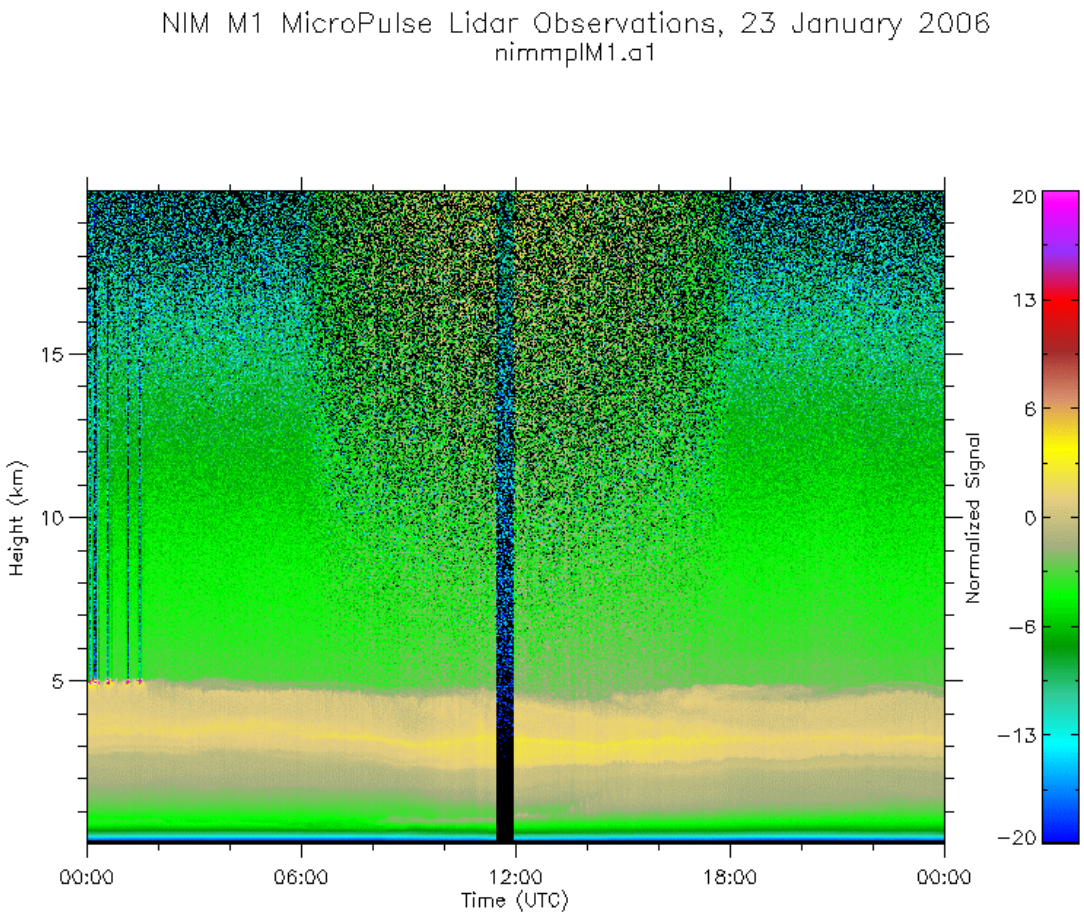

Figure 6. Time-height cross-section of range-normalized backscatter from the AMF MPL data on 23 January 2006 in Niamey, Niger, Africa. The warm colors in the lower 5-km of the atmosphere are indicative of dust and biomass burning aerosol. The striations indicate boundaries between layers of aerosol with different light scattering properties at 523-nm, which is the MPL wavelength.

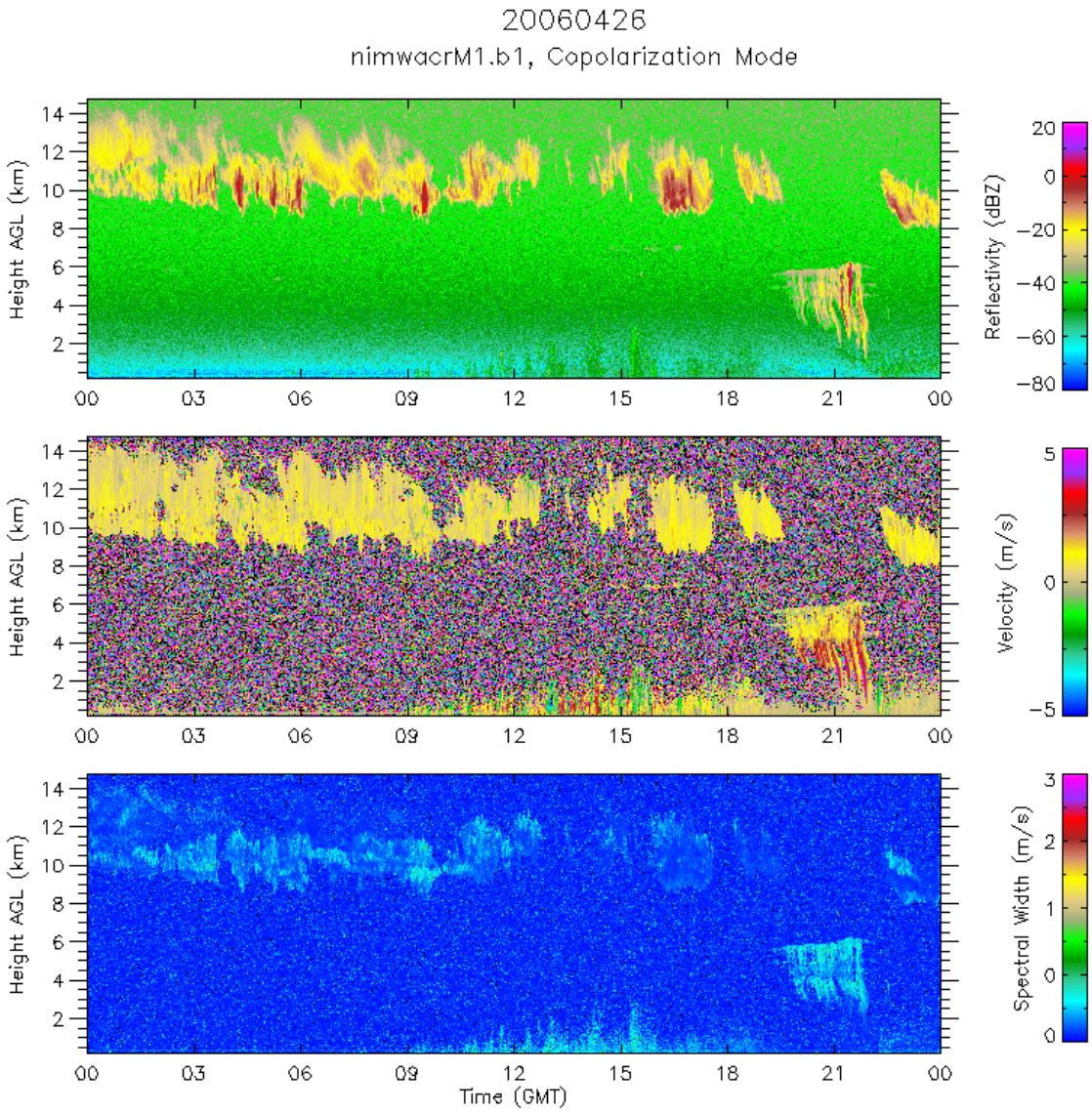

Figure 7. Time-height cross-section from 26 April 2006 of the range normalized effective reflectivity factor in units of dBZ, Doppler velocity in units of ms^{-1}, and Doppler velocity spectral width in units of ms^{-1}. Echoes extending from the surface to approximately 2-km during the daytime are probably due to a combination of dust, refractive turbulence, and insects.